Homogeneous nucleation of quark-gluon plasma, finite size effects, and long-lived metastable objects

E. E. Zabrodin,[1,2] L. V. Bravina,[1,2] H. Stöcker,[1] and W. Greiner[1]
[1]*Institute for Theoretical Physics, University of Frankfurt, Robert-Mayer-Str. 8-10, D-60054 Frankfurt, Germany*
[2]*Institute for Nuclear Physics, Moscow State University, 119899 Moscow, Russia*
(Received 6 May 1998)

The general formalism of homogeneous nucleation theory is applied to study the hadronization pattern of the ultrarelativistic quark-gluon plasma (QGP) undergoing a first order phase transition. A coalescence model is proposed to describe the evolution dynamics of hadronic clusters produced in the nucleation process. The size distribution of the nucleated clusters is important for the description of the plasma conversion. The model is most sensitive to the initial conditions of the QGP thermalization, time evolution of the energy density, and the interfacial energy of the plasma-hadronic matter interface. The rapidly expanding QGP is first supercooled by about $\Delta T = T - T_c = 4-6$ %. Then it reheats again up to the critical temperature T_c. Finally it breaks up into hadronic clusters and small droplets of plasma. This fast dynamics occurs within the first 5–10 fm/c. The finite size effects and fluctuations near the critical temperature are studied. It is shown that a drop of longitudinally expanding QGP of the transverse radius below 4.5 fm can display a long-lived metastability. However, both in the rapid and in the delayed hadronization scenarios, the bulk pion yield is emitted by sources as large as 3–4.5 fm. This may be detected experimentally both by a Hanbury–Brown-Twiss interferometry signal and by the analysis of the rapidity distributions of particles in narrow p_T intervals at small $|p_T|$ on an event-by-event basis. [S0556-2813(99)07502-0]

PACS number(s): 12.38.Mh, 24.10.Pa, 25.75.−q, 64.60.Qb

I. INTRODUCTION

The hadronization of quark-gluon plasma (QGP) possibly produced in the early Universe or in ultrarelativistic heavy ion collisions has received much activity during the last decades [1–21]. Despite significant progress in the understanding of the variety of possible signals and features of the QGP, the nature of the phase transition (PT) between deconfined and confined phases is not clear yet. Assuming a first order PT, usually an adiabatic scenario is invoked to describe the conversion of plasma into hadrons. A few years ago, in [15] it was pointed out that the coarse-grained field theory of homogeneous nucleation [22,23] can be relevant for the relativistic PT also. This scenario assumes the nucleation of hadronic bubbles, e.g., bubbles of pion gas, within the (initially homogeneous) supercooled metastable QGP as the starting point of the PT. These bubbles are nucleated because of the thermodynamic fluctuations of the energy density in the system. Then bubbles with radii smaller than the critical radius R_c shrink and bubbles of critical size are in metastable equilibrium, while bubbles with radii larger than R_c gain in size and develop into the new phase. The treatment of the relaxation of the metastable state within the framework of the nucleation theory provides the fundamental nucleation rate [23–25], which expresses the number of viable nucleating clusters of the new phase via the equilibrium number of critically large clusters.

Langer's theory has been applied [16,17] to calculate the hadronization of rapidly expanding baryon-free QGP, produced in heavy ion collisions at RHIC and LHC energies. Although this approach seems to be more realistic than the idealized adiabatic PT, several questions remain open: These calculations [17] have shown that the latent heat released during the plasma conversion is not sufficient to prevent the strong (20–35 %) supercooling of the system. Thus, the rapidly quenched system leaves the region of metastability and enters the highly unstable spinodal region. Here the theory of spinodal decomposition might be in order to describe the further evolution of the fluctuations leading to the breakup of that system.

Second, since the critical radius drops quickly when the temperature is lowered, the bulk creation of the hadronic phase should begin [16] when the bubble radii are $r \leqslant 0.8$ fm. Finally, in the nonscaling scenario the bubbles grow independently of the total expanding volume. Then the completion of the PT will be significantly delayed [17]. Even within the scaling scenario the time necessary for the completion of the PT varies from 50 to 90 fm/c (depending strongly on the numerical value of the surface tension).

Hence, from the above one may conclude that either (i) the homogeneous nucleation scheme is inappropriate to describe the hadronization of relativistic systems or (ii) that some important features of the first order PT are still missing. The situation would change if it turned out that the amount of plasma converted into hadrons had been underestimated in earlier works.

Recently, the calculation of the dynamical factor κ governing the growth rate of subcritical bubbles was reexamined [26], and the size distribution of bubbles in configuration space has been used to estimate the supercooling of rapidly expanding QGP [27]. The latter plays an important role in the hadronization of plasma produced in relativistic collisions. When the critical radius of hadronic bubbles drops due to the rapid fall of the temperature in the expanding system,

the subcritical bubbles transfer to the region of supercritical sizes for these new conditions in the system. These bubbles then stop to shrink and start to gain size, thus increasing the total volume of the hadronic phase.

In the present paper we study the effect of the bubble size distribution on the dynamics of the plasma-hadrons phase transition. The paper is organized as follows: the model used to study the QGP hadronization is described in Sec. II. Section III reviews the formalism of nucleation theory. The evaluation of both dynamical and statistical prefactors appearing in Langer's theory is discussed. A coalescence-type model for the further evolution of the nucleated hadronic bubbles is proposed. The role of initial conditions (as well as effects of variations of the model parameters, i.e., the value of the surface tension, the minimum size of the pionic bubbles, the nonscaling regime and dilution factor, the prefactors, etc.) on the relaxation of the metastable QGP is studied in Sec. IV. Section V presents the investigation of the finite size effects, the creation of long-lived states with metastable QGP and hadronic bubbles, and temperature fluctuations in the system. Finally, the results are summarized in the Conclusions.

II. MODEL

We consider a QGP produced in collisions of two heavy ions at RHIC or LHC energies. It is assumed that the plasma is thermalized soon. A wide range of initial conditions is studied; see Sec. IV. The expansion and cooling is ruled by relativistic hydrodynamics.

When the plasma cools below the critical temperature T_c, a first order phase transition is initiated by the appearance of hadronic bubbles. The bag model equation of state (EOS) for the QGP consisting of gluons and massless quarks reads

$$p_q=\frac{\pi^2}{90}\left(16+\frac{21}{2}n_f\right)T^4-B=a_qT^4-B, \tag{1}$$

with the number of flavors, n_f, and bag constant B. The EOS of the relativistic pion gas is

$$p_h=\frac{\pi^2}{10}T^4=a_hT^4. \tag{2}$$

By imposing the condition $p_q=p_h$ at $T=T_c$ one may find the critical temperature

$$T_c=\left(\frac{B}{a_q-a_h}\right)^{1/4}. \tag{3}$$

For a two-flavored QGP with $B^{1/4}=235$ MeV [15] this gives $T_c=169$ MeV.

The total energy density of the mixed quark-hadron phase, e, can be treated in the capillary (thin wall) approximation as a linear combination of the energy density of the hadronic phase, e_h, in the fraction of the volume occupied by hadronic bubbles, $h=V_h/V_{\rm tot}$, the energy density of the QGP, e_q, in the rest of the volume $V_q=(1-h)V_{\rm tot}$, and the energy density of the quark-hadronic interface, $e_S=\sigma S_h/V_{\rm tot}$:

$$e=he_h+(1-h)e_q+\sigma\frac{S_h}{V_{\rm tot}}. \tag{4}$$

Here σ is the surface tension of the interface between the two phases. The last term in Eq. (4) is usually disregarded [15–17] though its contribution to the total energy density may be comparable with the other two: the ratio of the interface between the phases to the hadronic volume is not too small. For instance, assume that all bubbles are of the same radius, $|R|=\alpha$. Then, at $\sigma=0.1T_c^3$ [28] the surface energy density scales as $e_S\approx\alpha^{-1}e_h$. Therefore, the surface term in Eq. (4) may be omitted only for sufficiently large ($r\geqslant 4$ fm) hadronic clusters.

Similarly to the energy density, the total pressure also consists of three terms

$$p=hp_h+(1-h)p_q+\sum c_ip_L^{(i)}, \tag{5}$$

where the pressure of the spherical surface of radius R_i is given by the Laplace formula, $p_L^{(i)}=2\sigma/R_i$, and c_i is the local concentration of bubbles of radius R_i in the total volume.

The Bjorken model [3] of scaling longitudinal expansion is applied to find the time evolution of the energy density. It yields the derivative of the energy density with respect to the proper time τ,

$$\frac{de}{d\tau}=-\frac{e+p}{\tau}. \tag{6}$$

Next one needs to compute the fraction of the total volume converted to hadronic phase. The pionic bubbles, appearing because of the fluctuations in the energy density, will either shrink or grow. This problem cannot been solved on the basis of the thermodynamic theory of fluctuations only. It requires a kinetic description of the process of bubble evolution. The volume fraction $h(R,t)$ of bubbles of size R at time t obeys the equation of motion in size space

$$\frac{\partial h(R,t)}{\partial t}=-\frac{\partial}{\partial R}[v(R)h(R,t)]+h^{\rm nucl}(R,t), \tag{7}$$

where $v(R)$ is the radial velocity and $h^{\rm nucl}$ denotes the hadronic fraction created at time t. Without the nucleation term Eq. (7) transforms into the continuity equation of the Lifshitz-Slyozov theory [30]. The volume fraction $h^{\rm nucl}(R)$ of bubbles of size R nucleated per unit time is given [31] by the distribution

$$h^{\rm nucl}(R)=\frac{I}{\sqrt{2\pi(9\tau+2\lambda_Z^2)}}\exp\left[\frac{9\tau+2\lambda_Z^2}{2}(r-1)^2\right]\times\int_r^\infty a[3\tau(a^2+a+1)+2\lambda_Z^2a^2]\times\exp\left[-\frac{9\tau+2\lambda_Z^2}{2}(a-1)^2\right]da, \tag{8}$$

containing the nucleation rate I, the critical exponent τ, and the two dimensionless variables λ_Z and r (see below), so that

$$\int_0^\infty h^{\mathrm{nucl}}(R)dR = I. \tag{9}$$

Instead of using a continuous spectrum, hadronic matter in our model is represented by a discrete spectrum of pion bubbles starting from $r_0 = 1$ fm.

III. THEORY OF HOMOGENEOUS NUCLEATION

Homogeneous nucleation has been the subject of intensive investigation both theoretically and experimentally for a long period (for reviews see [32–34] and references therein). In our analysis we follow the coarse-grained theory by Langer [22,23], who extended the classical Becker-Döring-Zeldovich (BDZ) theory of nucleation [35,36] to field theories. The nucleation rate in both classical and modern coarse-grained field theories reads

$$I = I_0 \exp\left(-\frac{\Delta F_c}{T} \right). \tag{10}$$

Here I_0 is the preexponential factor and ΔF_c is the excess free energy of the critical cluster in the system. In Langer's theory the prefactor I_0 is a product of a dynamical and a statistical prefactor, κ and Ω_0, respectively

$$I_0 = \frac{\kappa}{2\pi}\Omega_0. \tag{11}$$

It is interesting that under certain assumptions the prefactor derived in the classical theory may be obtained [37] identical to that of the modern theory.

To clarify the meaning of both the dynamical and the statistical prefactors, let us consider a classical system with N degrees of freedom described by a set of N collective coordinates η, $i = 1, \ldots, N$. The coarse-grained free energy functional $F\{\eta\}$ of the system has local minima $F\{\eta_i\}$ in the $\{\eta\}$ space, corresponding to metastable and stable states, separated by the energy barrier. The point of minimal energy along the barrier is the so-called saddle point $\{\eta^S\}$. Note that this saddle-point configuration corresponds to the critical cluster of a condensing phase in the classical theory. In contrast, in field theory the critical cluster of a condensing phase may not necessarily be a physical object but rather corresponds to a certain saddle-point configuration in phase space. The phase transition occurs when the configuration $\{\eta_i\}$ moves from the vicinity of a metastable minimum to the vicinity of a stable one. When the potential barrier is overcome, it is most likely for the trajectory of the system to pass across a small area around the intermediate saddle point $\{\eta^S\}$. The rate of the decay of the metastable state is determined by the steady-state current across the saddle point from the metastable to the stable minimum of $F\{\eta\}$.

Performing a Taylor series expansion of $F\{\eta\}$ around the $\{\eta^S\}$ and keeping only quadratic terms yields

$$F\{\eta\} - F\{\eta^S\} = \frac{1}{2}\sum_{k=1}^{N} \lambda_k (\eta_k - \eta_k^S)^2, \tag{12}$$

where λ_k are the eigenvalues of the matrix $M_{ij} = \partial^2 F/\partial\eta_i \partial\eta_j$, evaluated at the saddle point. By definition, at $\{\eta^S\}$ the free energy density functional reaches its local maximum. Therefore, at least one of the eigenvalues λ_k must be negative. Following Langer, we denote it as λ_1. Then one may approximate the potential barrier between the metastable and stable states well by the excess of the Helmholtz free energy, ΔF, corresponding to the formation of a spherical bubble of size R. In the thin wall approximation, ΔF is the sum of the bulk and the surface energies,

$$\Delta F(R) = -\frac{4\pi}{3}R^3 \Delta p + 4\pi R^2 \sigma, \tag{13}$$

with Δp being the difference in pressures inside and outside of the bubble. In the droplet model of Fisher [38], the activation free energy includes also the so-called curvature term. It arises due to small fluctuations in the shape of the bubble, which leave unchanged both the volume and the surface area of the bubble,

$$\Delta F^F(R) = -\frac{4}{3}\pi R^3 \Delta p + 4\pi\sigma R^2 + 3\tau T \ln\frac{R}{r_0}. \tag{14}$$

Here $\tau \approx 2.2$ is the Fisher critical exponent and r_0 is the radius of the smallest bubble in the system. Minimization of ΔF with respect to the radius R yields the free energy of the critical bubble:

$$\Delta F_c^F = \frac{4}{3}\pi R_c^2 \sigma + \tau T\left(3\ln\frac{R_c}{r_0} - 1 \right). \tag{15}$$

Here the critical radius R_c should be evaluated by solving the equation $\partial \Delta F^F/\partial R = 0$.

It is convenient to introduce new variables [39]: the similarity number $\lambda_Z = R_c\sqrt{4\pi\sigma/T}$ and the reduced radius $r = R/R_c$. In terms of these variables we have

$$\frac{\Delta F_c^F}{T} = -\tau + \frac{\lambda_Z^2}{3} + 3\tau \ln\frac{R_c^F}{r_0}, \tag{16}$$

$$\frac{\Delta F^F}{T} = -\left(\tau + \frac{2}{3}\lambda_Z^2 \right) r^3 + \lambda_Z^2 r^2 + 3\tau \ln\frac{R_c^F}{r_0}. \tag{17}$$

In the harmonic approximation for the activation energy of a bubble near the critical radius, Eq. (17) reads

$$\frac{\Delta F^F}{T} = \left(\frac{\Delta F^F}{T} \right)_{R=R_c} + \frac{1}{2T}\left(\frac{\partial^2 \Delta F^F}{\partial R^2} \right)_{R=R_c} (R - R_c)^2$$

$$= \frac{\Delta F_c^F}{T} - \frac{9\tau + 2\lambda_Z^2}{2}(r-1)^2, \tag{18}$$

and we get finally, for the only negative eigenvalue λ_1,

$$\lambda_1 = -T(9\tau + 2\lambda_Z^2). \tag{19}$$

This expression will be used to determine the nucleation rate of the process, in particular the statistical prefactor.

A. Dynamical prefactor

The dynamical prefactor $\kappa = d/dt[\ln(R-R_c)]$, which is related to the single negative eigenvalue λ_1, determines the growth rate of the critical bubble of size R_c at the saddle point. To compute κ one has to solve the hydrodynamic equations [15,40] which describe the growth of a bubble of the hadronic phase due to the diffusion flux through the interface.

For a baryon-free plasma, where the thermal conductivity is absent because of the absence of a rest frame defined by the baryon net charge, the dynamical prefactor has been calculated by Csernai and Kapusta [15] to be

$$\kappa_1 = \frac{4\sigma\left(\zeta + \frac{4}{3}\eta\right)}{(\Delta\omega)^2 R_c^3}, \tag{20}$$

containing the bulk and the shear viscosities ζ and η, and the difference $\Delta\omega$ between the enthalpy densities of the plasma and hadronic phase, $\omega = e + p$.

Here it is implied that the energy flow $\omega\vec{v}$, where $\vec{v}$ is the velocity of the net particles, is provided by viscous effects. Recently Ruggeri and Friedman [26] argued that the energy flow does not vanish even in the absence of heat conduction. Since the change of the energy density e in time is given in the low velocity limit by the conservation equation

$$\frac{\partial e}{\partial t} = -\nabla\cdot(\omega\vec{v}), \tag{21}$$

this means that the energy flow $\propto\omega\vec{v}$ is always present. Then the calculation of the dynamical prefactor for a system with zero thermal conductivity leads to the expression

$$\kappa_2 = \left(\frac{2\sigma\omega_q}{R_c^3(\Delta\omega)^2}\right)^{1/2}, \tag{22}$$

which agrees with the result of [42] obtained for nonviscous systems; i.e., the viscous effects cause only small perturbations to Eq. (22). Note that the dynamical prefactor κ_2 might violate the dynamical scaling laws of Kawasaki [43] in the vicinity of the critical point (for details see [40,42,43]) and, therefore, should be handled with great care.

Figure 1 shows the evolution of the dynamical prefactors κ_1 and κ_2 below the critical temperature for different values of the surface tension. To calculate κ_1 we use the fact that the shear viscosity of a two-flavored QGP, $\eta = 1.29T^3/[\alpha_S^2\ln(1/\alpha_S)]$ [41], is much larger as compared with the bulk viscosity ζ. One can see that Eq. (22) predicts higher rates κ for moderate or weak supercooling. It means, in particular, that the minimal temperature, reached by the system during the cooling stage, should be higher if κ_2 is used in the calculations rather than κ_1. We will discuss the effect of the replacement of the dynamical prefactor on the course of the plasma hadronization in the model in Sec. IV.

Homogeneous nucleation theory permits us also to determine the macroscopic radial velocity of bubbles [37] via the dynamical prefactor κ and the critical radius R_c. Assuming that bubbles of hadronic phase grow due to the diffusion flux through their interface, we have

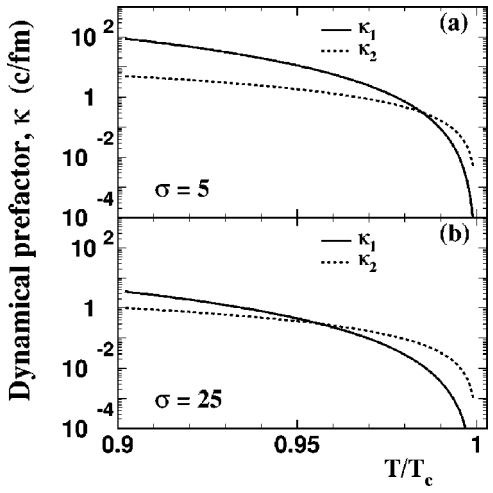

FIG. 1. Dynamical prefactors κ_1 (solid line) and κ_2 (dashed line) calculated with $\sigma = 5$ MeV/fm^2 (a) and $\sigma = 25$ MeV/fm^2 (b) vs the temperature of the system.

$$v(R) \equiv \frac{dR}{dt} = |\kappa|\left(\frac{R_c}{R}\right)^2 (R - R_c). \tag{23}$$

If $R = R_c$, the radial velocity drops to zero and the bubble is in (metastable) equilibrium. If $R < R_c$, $v(R)$ is negative and, hence, the bubble collapses. If $R > R_c$, the radial velocity is positive and the bubble grows.

B. Statistical prefactor

The statistical prefactor Ω_0 is a measure of the volume of the saddle-point region in phase space available for nucleation. Sometimes Ω_0 is called also a generalization of the Zeldovich factor Z [32], although this is a crude simplification, since the relation between these two factors is actually more complex [37]. The product of Ω_0 and the exponential $\exp(-\Delta F_c/T)$ gives the probability of finding the system at the saddle point—rather than at the metastable configuration.

According to [22–25], the statistical prefactor can be written as

$$\Omega_0 = \mathcal{V}\left(\frac{2\pi T}{|\lambda_1|}\right)^{1/2}\left[\frac{\det(M_0/2\pi T)}{\det(M'/2\pi T)}\right]^{1/2}, \tag{24}$$

where $\mathcal{V}$ is the available phase space volume at the saddle point, the index ''0'' denotes the metastable state, and the prime indicates that the negative eigenvalue λ_1, as well as the zero eigenvalues of the matrix M_{ij}, is omitted.

The calculation of the fluctuation determinant in Eq. (24) is usually extremely difficult and, moreover, a very important uncertainty exists in the determination of Ω_0. Indeed, in the harmonic approximation (12) for the free energy density functional $F\{\eta\}$,

$$\Omega_0 = \mathcal{V}\left(\frac{2\pi T}{|\lambda_1|}\right)^{1/2}\prod_{l=l_0+2}^{N}\left(\frac{2\pi T}{\lambda_l^{(S)}}\right)^{1/2}\prod_{l=1}^{N}\left(\frac{\lambda_l^{(0)}}{2\pi T}\right)^{1/2}. \tag{25}$$

Here $\lambda_l^{(S)}$ and $\lambda_l^{(0)}$ are eigenvalues of the mobility matrix M, evaluated at the saddle point and at the metastable point, respectively, and l_0 is the total number of symmetries of $\{F\}$

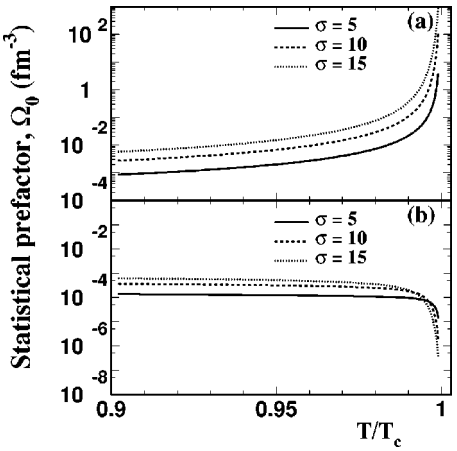

FIG. 2. (a) Statistical prefactor Ω_0 given by Eq. (30) vs temperature with $\sigma=5$ (solid line), 10 (dashed line), and 15 (dotted line) MeV/fm^2. (b) The same as (a) but for Eq. (29).

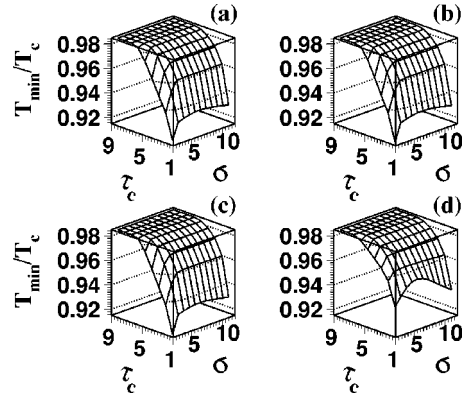

FIG. 3. Supercooling of the system as function of critical time τ_c and surface tension σ. (a) Bubbles grow together with the total volume (scaling regime); entropy of the bubble surface is neglected. (b) Bubbles grow independently on the total volume (nonscaling regime); entropy of the bubble surface is neglected. (c) Nonscaling regime, surface entropy is taken into account. (d) The same as (c), but prefactor κ_1 is substituted by κ_2.

which are broken by the presence of the saddle-point configuration. Since it is the translational symmetry of the system that is broken due to bubble creation, the three translation invariance zero modes omitted in the fluctuation determinant give rise to the prefactor proportional to $\lambda_1^{-3/2}$ in the expression for the available phase space volume $\mathcal{V}$:

$$\mathcal{V}=V\left(\frac{8\pi\sigma}{3|\lambda_1|}\right)^{3/2}. \tag{26}$$

Here V is the total volume of the system. In [23] the fluctuation corrections in the products over $\lambda_l^{(S)}$ and $\lambda_l^{(0)}$ from Eq. (25) are absorbed into the free energy of the metastable region and the saddle-point region, namely,

$$\exp(-F_0/T)\equiv\exp(-F\{\eta^0\}/T)\prod_{l=1}^{N}\left(\frac{2\pi T}{\lambda_l^{(0)}}\right)^{1/2}, \tag{27}$$

$$\exp(-F_S/T)\equiv\exp(-F\{\eta^S\}/T)\prod_{l=l_0+2}^{N}\left(\frac{2\pi T}{\lambda_l^{(S)}}\right)^{1/2}. \tag{28}$$

Therefore, the activation energy of a critical cluster is simply $\Delta F_c=F_S-F_0$ and

$$\Omega_0=V\frac{32\pi^2T^{1/2}}{|\lambda_1|^2}\left(\frac{\sigma}{3}\right)^{3/2}. \tag{29}$$

In Ref. [42] it was mentioned that there are four more terms in the product over $\lambda_l^{(0)}$ than in that over $\lambda_l^{(S)}$. Therefore, the free energy difference can not be precisely a logarithm of these products. The final expression for the statistical prefactor, which accounts for the four unpaired $\lambda_l^{(0)}$ modes, reads

$$\Omega_0=\frac{2}{3\sqrt{3}}\frac{V}{\xi^3}\left(\frac{\sigma\xi^2}{T}\right)^{3/2}\left(\frac{R_c}{\xi}\right)^4, \tag{30}$$

where ξ is the correlation length.

The statistical prefactors corresponding to the expressions (29) and (30) are shown in Fig. 2. In contrast to the curves in the lower panel, the curves in the upper panel diverge at $T=T_c$. This is an unphysical result, which is due to the fact that the nucleation process is turned off as $T\to T_c$. It is worth noting, however, that the rise of Ω_0 is counterbalanced by the factor $\exp(-\Delta F_c/T)$, which drops to zero at the critical temperature. Therefore, the total nucleation rate will increase with dropping temperature for both prefactors. Also, the correlation length ξ is not a constant, but rather scales with the temperature in the proximity of the critical point, where the PT turns to second order, as $\xi(T)=\xi(0)(1-T_{\rm crit}/T)^{-\nu}$, with the critical exponent $\nu=0.63$ [42]. Since such a critical point does not exist in the plasma to hadron gas phase transition scheme presented here, Eq. (29) is used to calculate the statistical prefactor Ω_0.

IV. RELAXATION OF THE METASTABLE QGP

As in any phenomenological model, the scenario of a homogeneously nucleating QGP is based on a set of model parameters. Here, the role of each parameter for the dynamics of the PT is studied in order to reveal those most relevant parameters to which the model results are most sensitive.

The theory of homogeneous nucleation is valid for systems which are not too far from equilibrium. In particular, the supercooling in the system should not be too strong—otherwise the nucleation theory fails. The minimum temperature reached by the expanding and cooling plasma is shown in Fig. 3 as a function of the surface tension σ and the critical time τ_c. The most reliable value of the surface tension lies within the range $0.015\leqslant\sigma/T_c\leqslant0.1$ [28,44], i.e., $2\leqslant\sigma\leqslant12.5$ MeV/fm^2 for the given T_c. Note that even in the case of an extremely fast expansion and very low values of σ, the supercooling of the system does not exceed 8%. This result does practically not change when bubbles grow independently in the nonscaling regime on the growing total volume [Fig. 3(b)]. Even when the surface tension and pressure of the bubble surface are included in the expressions for total energy density and pressure, Eqs. (4) and (5) [Fig. 3(c)], the results stay put.

If the dynamical prefactor given by Eq. (20) is replaced

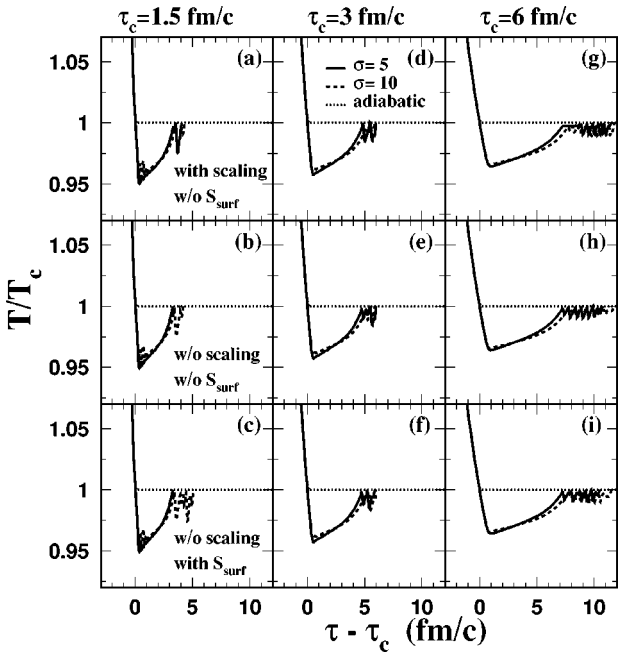

FIG. 4. The temperature evolution with time for the expansion scenarios with $\tau_c = 1.5$ fm/c [(a)–(c)], 3 fm/c [(d)–(f)], and 6 fm/c [(g)–(i)]. The sequence of conditions within each subgroup of panels corresponds to that of Figs. 3(a)–3(c). The dotted curves are the idealized adiabatic scenario of the PT; the others show the result of solving of rate equations with $\sigma = 5$ (solid lines) and 10 (dashed lines) MeV/fm^2.

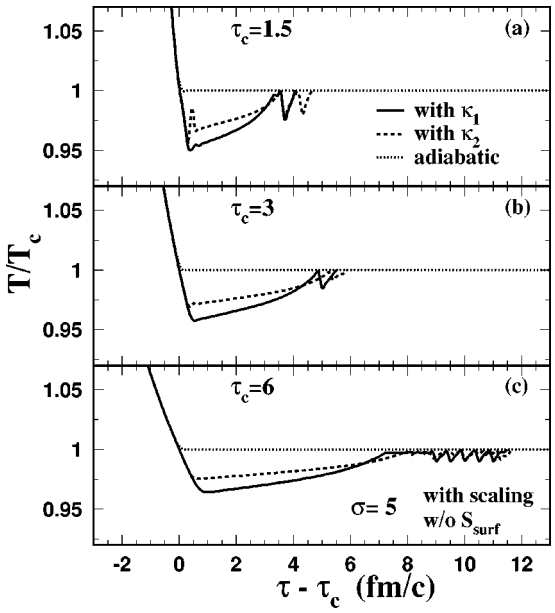

FIG. 5. (a)–(c) The same as Figs. 4(a), 4(d), 4(g) with $\sigma = 5$ MeV/fm^2 but for the solutions of the rate equations with κ_1 (solid lines) and with κ_2 (dashed lines).

by that of Eq. (22), the amount of QGP volume converted to hadrons at the earlier stages of the supercooling is increased. Thus, the supercooling of the system in the latter case is about 2% weaker [Fig. 3(d)] than that shown in Figs. 3(a)–3(c).

The analysis of the QGP equilibration times within the parton cascade model (PCM) by Geiger [45], which has been done for the RHIC and the LHC energies, yields the earliest equilibration time for the plasma as $\tau_{\rm init} = 3/8$ fm/c with $T_{\rm init} \approx 2T_c$. Then the critical temperature will be reached at $\tau_c = 3$ fm/c, which corresponds to a supercooling of about 5–6 % in our figures. Therefore, one may conclude that the application of the homogeneous nucleation theory to the hadronization process of even a relativistic expanding QGP seems quite reasonable.

The temperature is plotted as a function of the proper time τ in Fig. 4 for $\tau_c = 1.5$, 3, and 6 fm/c. The upper panels in this figure corresponds to conditions (a) of Fig. 3, the middle row corresponds to conditions (b), and the lower row corresponds to conditions (c) of the same figure. Hadronization causes the release of the latent heat, and the system reheats to temperatures close to T_c. Then the nucleation and growth of hadronic bubbles come to a halt.

The continuing increase of the total volume leads again to a decrease of the temperature, and the phase transition continues immediately. These oscillations of the temperature in the vicinity of T_c are well observable in Fig. 4. The mixed system is quite unstable at this stage, since any negligibly small rise of the temperature forces the system to reach the critical point, where, in turn, it may break up into fragments. Then the theory of spinodal decomposition might be relevant to describe the hadronization of the rest of the QGP. The time $\Delta\tau$ needed for the system (for $\sigma = 5$–10 MeV/fm^2) to reach the zone of the oscillations scales with τ_c as

$$\Delta\tau = 2.9\tau_c^{1/2}, \tag{31}$$

within the interval $1.5 \leqslant \tau_c \leqslant 9$ fm/c.

Changing the dynamical prefactor from κ_1 to κ_2 (Fig. 5) leads to negligibly small shifts in the time needed to reach the vicinity of the critical temperature. This is due to the fact that the late time evolution of the system is governed by the Lifshitz-Slyozov dynamics, which is generally much more important [30] for the course of a first order PT than the initial size distribution of clusters given by the nucleation theory.

Therefore, the model does not appear to be very sensitive to a nonscaling growth of the nucleated bubbles, to the incorporation of the surface entropy in the rate equations, and to the numerical values of the dynamical prefactors obtained within the range of model parameters applied. The most important parameters are the value of the surface tension σ and the time to reach of the transition temperature, τ_c, which is determined by the initial conditions and by the expansion dynamics of the system. The effects of varying just these two factors for the relaxation process of the metastable QGP are studied below.

From Fig. 6 one may conclude that, at the very beginning of the phase transition, the process of bubble nucleation is the main mechanism of plasma conversion. The creation of the new phase reaches its saturation value soon after 0.5–1.5 fm/c, and the growth of the total hadronic fraction of the total volume proceeds due to the diffusion growth of already nucleated bubbles. Both the nucleation and the diffusion process contribute (almost equally) to the hadronization of the QGP.

The critical radius in the system initially drops to about 1 fm (Fig. 7); then, as a result of reheating, it rises up to $R_c \approx 2-4$ fm. Then the oscillations begin. At $T = T_c$, the criti-

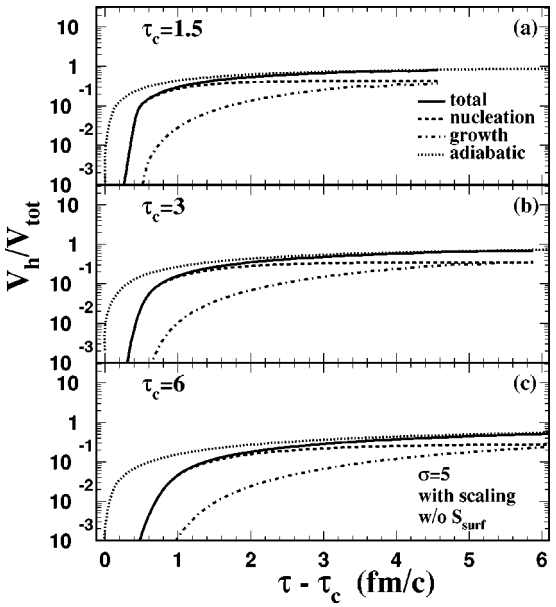

FIG. 6. The part of the QGP volume converted into hadrons for the idealized adiabatic PT (dotted lines) and for homogeneous nucleation scenario with $\sigma=5$ MeV/fm^2. Solid lines correspond to the total volume fractions of hadronic matter, dashed lines denote the increase of hadronic volume due to the nucleation of new bubbles, and dash-dotted lines indicate the enlargement of the hadronic bubbles due to diffusion.

cal radius is, of course, infinite. The weak changes of the temperature near the critical point cause significant oscillations in the value of the critical radius which, in turn, are responsible for the irregularities in the size distribution of bubbles at the final stage of the PT (see Fig. 8, right lower panel). The radial oscillations of the intermediate-sized hadronic bubbles can result in the pulsed emission of matter and radiation owing to the strong acceleration and deceleration of

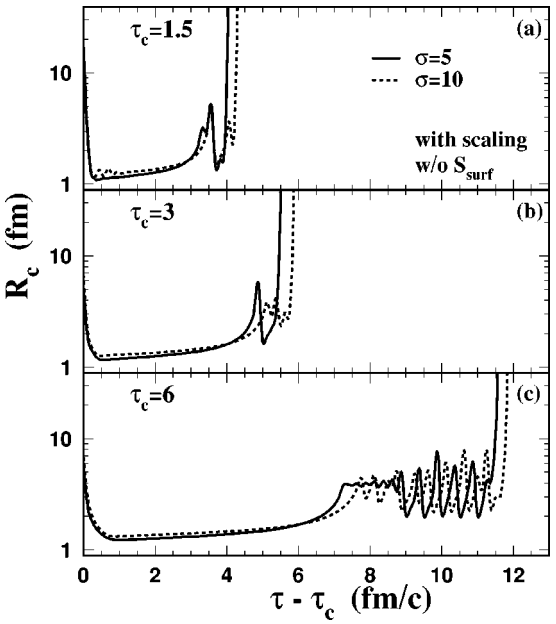

FIG. 7. Change of the critical radius as a function of time $\tau-\tau_c$ for the expanding system with $\tau_c=1.5$ (a), 3 (b), and 6 (c) fm/c, with $\sigma=5$ (solid lines) and 10 (dashed lines) MeV/fm^2.

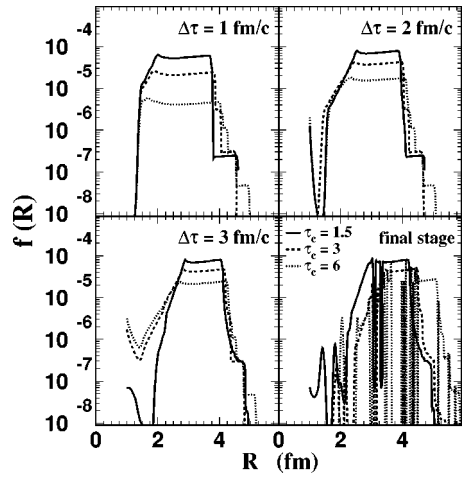

FIG. 8. Size distribution of hadronic bubbles at $\Delta\tau=1$, 2, and 3 fm/c after the beginning of the nucleation, and at the freeze-out for $\tau=1.5$, $\Delta\tau=4$ fm/c (solid curves), $\tau=3$, $\Delta\tau=6$ fm/c (dashed curves), and $\tau=6$, $2\Delta\tau=11.5$ fm/c (dotted curves).

matter in the vicinity of the bubble surface. These oscillations are analogous to the pulsations of a hot quark blob, discussed in [29]. Note, also, that bubble pulsations, occurring in the medium, generate sonic waves in the expanding plasma, but a discussion of this topic lies outside of scope of this paper.

When the nucleation just begins, the size distribution of hadronic bubbles shown in Fig. 8 has a characteristic plateaulike profile. At $\Delta\tau=1$ fm/c, just after entering the metastable region, the critical radius drops to its minimal value of about 1 fm. Then practically all bubbles are growing. Reheating of the system leads to a rise of the value of the critical radius. As a result, a noticeable fraction of shrinking bubbles appears. The central plateau becomes narrower, also because of the increase of bubble density per unit of radial interval. At the end of the homogeneous nucleation stage, as mentioned above, dips and peaks in the bubble size distribution arise due to the temperature oscillations. Note that the bubble size distribution established in the first order PT deviates clearly from the power-law distribution $f(A)\propto A^{-\tau}$ (A being the size of a cluster), which is typical for the second order PT.

The scaling of the change of the average radius of the hadronic bubbles with time (Fig. 9) demonstrates that the average radius depends mainly on the duration of the phase transition, but not on the expansion scenario. Since the nucleation of new bubbles is turned off after $\tau_0\approx1.2$ fm/c, we fit the distribution to the power law

$$\langle R(\tau)\rangle-\langle R(\tau_0)\rangle=\text{const}\times(\tau-\tau_0)^{1/3}, \tag{32}$$

with $R(\tau_0)=3$ fm, which is the Lifshitz-Slyozov (LS) $t^{1/3}$ law [30] of the coalescence process. We see that at the coalescence stage of the plasma conversion the agreement with the LS law is good. The deviations from this law at the late stage of the hadronization of QGP are also caused by the temperature fluctuations.

Finally, the dependence of the results on the minimum radius of the nucleated bubbles is studied. The upper panel of Fig. 10 depicts the temperature curves calculated with r_0

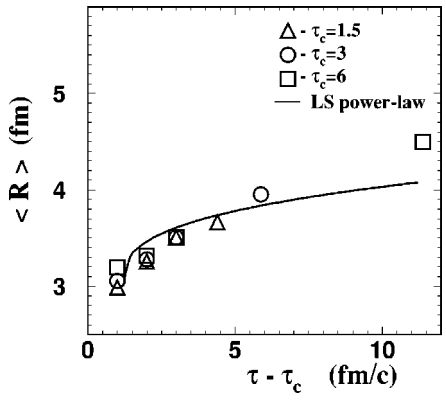

FIG. 9. Average radius of hadronic bubbles as a function of $\tau - \tau_c$ for the longitudinal expansion with $\sigma = 5$ MeV/fm^2 and with $\tau_c = 1.5$ (triangles), 3 (circles), and 6 (squares) fm/c. The solid curve is the fit to Lifshitz-Slyozov power law $\langle R \rangle \propto t^{1/3}$.

$=1$ and 2 fm, and the lower panel compares the size distributions of the bubbles at the end of the PT. Again one can see that the effect of the cutoff of small bubbles is negligible because of the rather broad initial distribution of bubbles in size space.

The results of this section may be summarized by concluding that the most important parameters of the model are the initial conditions, time $\tau_{\rm init}$ and temperature $T_{\rm init}$, of the QGP thermalization, as well as the scenario of further plasma expansion and the value of the surface tension σ. All other factors cause only small deviations from the solutions obtained with the fixed set of the aforementioned parameters. Note that effects like the final transients near the critical point are sensitively dependent on the fluctuations in the system, and these might (or might not) wash out these transients. Real systems produced in experiments with heavy ions are not infinite. Therefore, to complete our analysis, we have to clarify the role of the finite size effects.

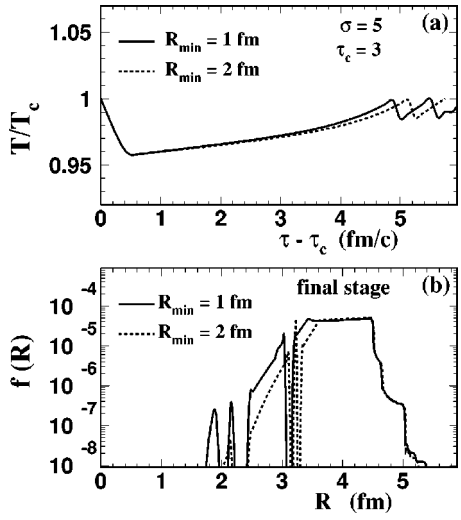

FIG. 10. (a) Temperature as a function of time for the expansion with $\sigma = 5$ MeV/fm^2 and $\tau_c = 3$ fm/c. Curves show the result of solving of rate equations with minimum radius of hadronic bubbles, $R_{\rm min} = 1$ (solid line) and 2 (dashed line) fm.

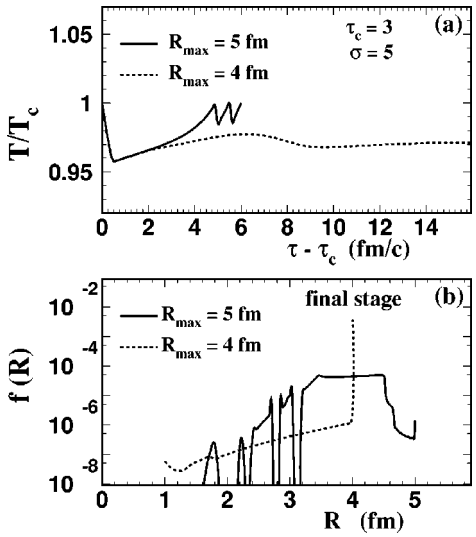

FIG. 11. Upper: the same as Fig. 10 but for maximum radius of hadronic bubbles $R_{\rm max} = 5$ (solid line) and 4 (dashed line) fm. Lower: size distributions of hadronic bubbles at the freeze-out for the same scenario as in upper panel with $R_{\rm max} = 5$ (solid line) and 4 (dashed line) fm.

V. ROLE OF FINITE SIZE EFFECTS

The biggest problem which has to be overcome before a careful investigation of the finite size effects can be tackled is the problem of the first order phase transition itself. Then, a consistent treatment of the finiteness of the system and, especially, of the surface induced phenomena is still an open question. Attempts to estimate the role of the finite size effects on the phase transitions in nuclear matter have been made in [46–48] on a basis of a purely thermodynamical picture of fluctuations. Can this approach be modified and applied for our kinetic analysis of the plasma hadronization? To answer the question note that the situation we face here may be subdivided into two cases.

First, let us imagine that a droplet of plasma is immersed into a hot gas of hadrons which acts as a heat bath; i.e., the temperature fluctuations in the droplet are suppressed. The compound system expands longitudinally, and the final size effects come into play via the finiteness of the transverse direction. The results obtained in Sec. IV are valid for central collisions of gold or lead ions ($R \geqslant 7$ fm) at relativistic energies. If then, by chance, the transverse radius of the expanding cylinder is smaller than 7 fm, the cutoff of large bubbles should reduce the volume fraction occupied by hadrons and affect the course of the phase transition. Figure 11 presents the evolution of both the temperature and the bubble size distribution as calculated with maximum radii of 5 fm and 4 fm, respectively. The behavior of the system differs drastically between these rather close values of R: as the central plateau in the size distribution lies within the range of $3 \leqslant r \leqslant 4.5$ fm at $t \approx 10$ fm/c, the cutoff of bubbles with $R > 5$ fm does not cause noticeable deviations from the scenario discussed in Sec. IV. However, for $R \leqslant 4$ fm the maximum temperature reached by the system during the reheating is reduced and the conversion of the QGP into hadrons is significantly delayed. As a result, the bubble size distribution has a pronounced peak at $R = 4$ fm (Fig. 11, lower panel).

The values of the cutoff radius, at which the slowly vary-

TABLE I. Maximum transverse radius of longitudinally expanding QGP at which the long-lived metastable state appears. The maximum temperature reached by the system during the plasma conversion is less than $0.98T_c$.

Surface tension σ (MeV/fm^2)	$\tau_c=1.5$ fm/c $R_{\max}$ (fm)	$\tau_c=3$ fm/c $R_{\max}$ (fm)	$\tau_c=6$ fm/c $R_{\max}$ (fm)
$T_c=150$ MeV			
2	3.64	3.96	4.35
5	3.70	4.25	4.63
10	3.85	4.35	4.76
$T_c=170$ MeV			
2	3.40	3.71	4.05
5	3.60	4.00	4.35
10	3.76	4.20	4.50
$T_c=200$ MeV			
2	3.13	3.37	3.69
5	3.23	3.60	3.98
10	3.39	3.79	4.20

ing temperature of the long-lived object does not exceed the $0.98T_c$ upper limit, are listed in Table I for various critical temperatures, surface tensions, and expansion rates. It is easy to see that all values are within the range of the central plateau in the bubble size distribution. Thus the most probable size of the emitting sources is not affected by the finiteness of the system.

For radii smaller than 2–3 fm, surface-induced effects must be taken into account. Undoubtedly, the theoretical treatment of the interface between plasma and hadronic matter is oversimplified as compared with realistic system. Therefore we are not able to make any quantitative predictions, based on the homogeneous nucleation theory, for the hadronization of such plasma filament.

Second and perhaps more realistic is the case of the formation of a plasma pattern as an isolated system, i.e., without any contact with a heat reservoir. Although the energy of the expanding system is conserved, fluctuations of the temperature [49] of the order of

$$\langle(\Delta T)^2\rangle=\frac{T^2}{C_V} \tag{33}$$

should occur. Here $C_V=(\partial E/\partial T)_V$ is the heat capacity at constant volume. For the two-component system consisting of QGP and hadronic matter, the temperature T is smeared around its mean value with width

$$(\langle(\Delta T)^2\rangle)^{1/2}=\frac{1}{2(TV)^{1/2}}\sqrt{\frac{1}{ha_h+(1-h)a_q}}. \tag{34}$$

The smaller the volume V of the system, the larger the temperature fluctuations and vice versa. Moreover, from Fig. 12 one may conclude that these fluctuations (at any given T) are larger in the hadronic system rather than that in the pure QGP phase. This is due to the smaller specific heat of the hadronic phase. We have seen in Sec. IV that—at temperatures of about $0.98T_c$ (or lower)—the critical radius and

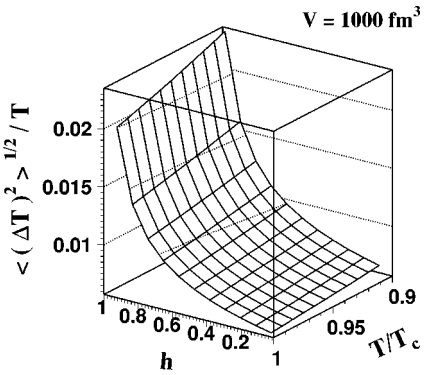

FIG. 12. Temperature fluctuations $(\langle(\Delta T)^2\rangle)^{1/2}/T$ as function of reduced temperature T/T_c and hadronic fraction h of the total volume of the system.

nucleation rate depend only very weakly on temperature variations within the range $\Delta T/T_c\approx 2\%$.

The situation changes completely when the temperature approaches the critical one. Since the hadronic matter here occupies already about 70% of the total volume, fluctuations of the temperature should be as large as 1% of T_c, i.e., 1.7 MeV for $V=10^3$ fm^3. For smaller volumes, say, 10 fm^3, the fluctuations rise to 10%, while for a volume as large as 16×10^3 fm^3 the width of the temperature smearing drops to 0.25% of T_c, still almost fully covering the range of the temperature fluctuations. Thus the expanding mixed system should breakup into fragments even earlier than in the scenario with the presence of heat bath. The conclusions drawn in Sec. IV remain true except for the appearance of irregularities in the size distribution of small and intermediate size hadronic bubbles.

VI. DISCUSSION AND CONCLUSIONS

It has been shown that the theory of homogeneous nucleation is applicable to describe the hadronization of a relativistically expanding quark-gluon plasma produced in heavy ion collisions. We have proposed a coalescence-type model to follow further the evolution of hadronic bubbles produced in a metastable QGP. The change of the average radius of the bubbles with time is shown to be consistent with the LS power law $\langle R\rangle\propto t^{1/3}$.

Various sets of model-dependent parameters are used to study the role of each of them on the course of the plasma-hadron PT. With rather good accuracy the number of these parameters may be reduced to the few main ones, namely, initial conditions of plasma thermalization, expansion scenario, and the value of the surface tension of the interface between plasma and hadronic matter. The supercooling of expanding QGP is found to be relatively moderate, 5–6 % only. Then the system reheats up to the critical temperature, where the temperature oscillations may occur. At $\Delta\tau=5-10$ fm/c after the beginning of the nucleation process (this time depends strongly on the initial conditions and model of expansion) the system hits the critical point. Since at that time already about 70–80 % of the total volume is occupied by hadronic matter and the system is dilute compare to initial state, the rest of the QGP may not be sufficient enough to ''glue'' the hadronic bubbles in a compound state.

The expanding system simply breaks up into fragments: hadronic clusters and small droplets of plasma. Because of finite size effects, the hadronization of QGP may be delayed and long-lived objects containing plasma and hadronic bubbles are produced. But the temperature fluctuations cause a broadening of the critical temperature region and earlier disintegration of the system. One has to appreciate, however, that using the given EOS it is impossible to get the conversion of total amount of QGP faster than that of the idealized adiabatic transition. It means that small sources like the QGP droplets will burst, emitting hadrons, from time to time up to about 40–50 fm/c, while the bulk amount of plasma is converted into hadrons within first 10 fm/c.

The entropy increase during the PT stage in the proposed scheme is small, 2–7 %, and there should be no significant changes in the integrated particle yields or pion to baryon ratios which can be detected experimentally. On the other hand, the formation of large clusters and their further disassembly will lead to significant multiplicity fluctuations in the rapidity spectra of secondary particles which should also have low transverse momenta. To search for these clusters experimentally one can examine the rapidity and azimuthal distribution in small p_T intervals, looking for islands in the sea of empty bins [50].

The nucleation process enforces the softening of the EOS and diminishes the transverse flow. Then, the cluster size distribution in the model discussed departs from a simple power-law falloff, which is expected for the second order PT. The most probable radius of emitting sources, which is fully determined by the evolution of the value of critical radius with temperature and by kinetics of the PT, varies from 3 fm to 4.5 fm. This signal may be checked by the analysis of data on Hanbury–Brown-Twiss (HBT) correlations. However, the rest of the plasma dispersed between the hadronic bubbles is hadronizing also, giving rise to a substantial yield of small bubbles. Therefore, the presence of a plateau in the range $R=3$–4.5 fm in the size distribution of hadronic clusters can be considered as a signal of the first order phase transition.

ACKNOWLEDGMENTS

We thank L.P. Csernai and M.I. Gorenstein for helpful discussions and valuable comments. L.B. and E.Z. are indebted to the Institute for Theoretical Physics at the University of Frankfurt for hospitality. This work was supported by the Graduiertenkolleg für Theoretische und Experimentelle Schwerionenphysik, Frankfurt–Giessen, the Bundesministerium für Bildung und Forschung, the Gesellschaft für Schwerionenforschung, Darmstadt, Deutsche Forschungsgemeinschaft, and the Alexander von Humboldt–Stiftung, Bonn.

[1] E.V. Shuryak, Phys. Rep. **61**, 71 (1980); Sov. J. Nucl. Phys. **16**, 220 (1973).
[2] F. Cooper, G. Frye, and E. Schönberg, Phys. Rev. D **11**, 192 (1974).
[3] J.D. Bjorken, Phys. Rev. D **27**, 140 (1983).
[4] E. Witten, Phys. Rev. D **30**, 272 (1984).
[5] H. Stöcker and W. Greiner, Phys. Rep. **137**, 277 (1986).
[6] R.B. Clare and D. Strottman, Phys. Rep. **141**, 177 (1986).
[7] P. Koch, B. Müller, and J. Rafelski, Phys. Rep. **142**, 167 (1986).
[8] H. von Gersdorff, L. McLerran, M. Kataja, and P.V. Ruuskanen, Phys. Rev. D **34**, 794 (1986).
[9] M. Gyulassy, K. Kajantie, H. Kurki-Suonio, and L. McLerran, Nucl. Phys. **B237**, 477 (1984).
[10] C. Greiner, P. Koch, and H. Stöcker, Phys. Rev. Lett. **58**, 1825 (1987).
[11] D.H. Rischke, B.L. Friman, B.M. Waldhauser, H. Stöcker, and W. Greiner, Phys. Rev. D **41**, 111 (1990).
[12] J.C. Miller and O. Pantano, Phys. Rev. D **42**, 3334 (1990).
[13] E.V. Shuryak, Phys. Rev. Lett. **68**, 3270 (1992).
[14] J.D. Bjorken, Int. J. Mod. Phys. A **7**, 4189 (1992).
[15] L.P. Csernai and J.I. Kapusta, Phys. Rev. D **46**, 1379 (1992).
[16] L.P. Csernai and J.I. Kapusta, Phys. Rev. Lett. **69**, 737 (1992).
[17] L.P. Csernai, J.I. Kapusta, Gy. Kluge, and E.E. Zabrodin, Z. Phys. C **58**, 453 (1993); E.E. Zabrodin, L.P. Csernai, J.I. Kapusta, and Gy. Kluge, Nucl. Phys. **A566**, 407 (1994).
[18] K. Geiger, Phys. Rev. D **51**, 3669 (1995).
[19] C.M. Hung and E.V. Shuryak, Phys. Rev. Lett. **75**, 4003 (1995).
[20] L. Rezzolla, J.C. Miller, and O. Pantano, Phys. Rev. D **52**, 3202 (1995).
[21] K. Werner and J. Aichelin, Phys. Rev. C **52**, 1584 (1995).
[22] J.S. Langer, Ann. Phys. (N.Y.) **41**, 108 (1967).
[23] J.S. Langer, Ann. Phys. (N.Y.) **54**, 258 (1969).
[24] C. Callan and S. Coleman, Phys. Rev. D **16**, 1762 (1977).
[25] I. Affleck, Phys. Rev. Lett. **46**, 388 (1981).
[26] F. Ruggeri and W.A. Friedman, Phys. Rev. D **53**, 6543 (1996).
[27] E.E. Zabrodin, L.V. Bravina, L.P. Csernai, H. Stöcker, and W. Greiner, Phys. Lett. B **423**, 373 (1998).
[28] Y. Iwasaki, K. Kanaya, L. Kärkkäinen, K. Rummukainen, and T. Yoshié, Phys. Rev. D **49**, 3540 (1994).
[29] H. Stöcker, G. Graebner, J.A. Maruhn, and W. Greiner, Phys. Lett. **95B**, 191 (1980); Z. Phys. A **295**, 401 (1980).
[30] I. Lifshitz and V. Slyozov, J. Phys. Chem. Solids **19**, 35 (1961); E.M. Lifshitz and L.P. Pitaevskii, *Physical Kinetics* (Pergamon, Oxford, 1981), Chap. 12.
[31] L.V. Bravina and E.E. Zabrodin, Phys. Rev. C **54**, 2493 (1996).
[32] J. Frenkel, *Kinetic Theory of Liquids* (Clarendon, Oxford, 1946), Chap. 7.
[33] J.D. Gunton, M. San Miguel, and P.S. Sahni, in *Phase Transitions and Critical Phenomena*, edited by C. Domb and J.L. Lebowitz (Academic, London, 1983), Vol. 8.
[34] K.F. Kelton, in *Solid State Physics*, edited by H. Ehrenreich and D. Turnbull (Academic, London, 1991), Vol. 45.
[35] R. Becker and W. Döring, Ann. Phys. (Leipzig) **24**, 719 (1935).
[36] Ya.B. Zeldovich, Acta Physicochim. URSS **18**, 1 (1943).
[37] L.V. Bravina and E.E. Zabrodin, Phys. Lett. A **233**, 423 (1997).
[38] M.E. Fisher, Physics (Long Island City, N.Y.) **3**, 255 (1967).

[39] L.V. Bravina and E.E. Zabrodin, Phys. Lett. A **202**, 61 (1995).
[40] L.A. Turski and J.S. Langer, Phys. Rev. A **22**, 2189 (1980).
[41] H. Heiselberg, Phys. Rev. D **49**, 4739 (1994); G. Baym, H. Monien, C.J. Pethick, and D.G. Ravenhall, Phys. Rev. Lett. **64**, 1867 (1990).
[42] J.S. Langer and L.A. Turski, Phys. Rev. A **8**, 3230 (1973).
[43] K. Kawasaki, J. Stat. Phys. **12**, 365 (1975).
[44] F. Karsch, B. Beinlich, J. Engels, R. Joswig, E. Laermann, A. Peikert, and B. Petersson, Nucl. Phys. B (Proc. Suppl.) **53**, 413 (1997).
[45] K. Geiger, Phys. Rev. D **46**, 4965 (1992); **46**, 4986 (1992).
[46] A.L. Goodman, J.I. Kapusta, and A.Z. Mekjian, Phys. Rev. C **30**, 851 (1984).
[47] L.P. Csernai and Z. Néda, Phys. Lett. B **337**, 25 (1994).
[48] C. Spieles, H. Stöcker, and C. Greiner, Phys. Rev. C **57**, 908 (1998).
[49] L.D. Landau, E.M. Lifshitz, and L.P. Pitaevskii, *Statistical Physics* (Pergamon, New York, 1980), Pt. 1.
[50] R.C. Hwa, C.S. Lam, and J. Pan, Phys. Rev. Lett. **72**, 820 (1994).